3. Klimenko, Yu.V. *Method of friction welding of metals*. USSR author's cert. 195846. Int. Cl. 23 B k 35/02. Publ. 04.05.67.
4. Thomas, W.M., Nicholas, E.D., Needham, J.C. *Friction stir butt welding*. Int. Pat. Appl. PCT/GB 92/02203. Publ. 1991.
5. Pietras, A., Zadroga, L. (2003) Rozwoj metody zdrzewania tarciowego z mieszaniem materialu zgrzeiny (FSW) i mozliwosci jej zastosowania. *Byuletyn Instytutu Spawalnictwa w Gliwicach*, **5**, 148–154.
6. Tsumura, T., Komazaki, T., Nakata, K. (2006) Structure and mechanical properties of ADC12 and A5083 dissimilar friction stir welded joints. *Transact. of JWRI*, **1**, 53–56.
7. Polovtsev, V.A., Shtrikman, M.M., Shilo, G.V. et al. (2005) Service characteristics of 1201 and AMg6 aluminium alloy joints made by friction welding. *Svarochn. Proizvodstvo*, **2**, 8–14.
8. Kluken, A., Ranes, M. (1995) Aluminium bridge constructions — welding technology and fatigue properties. *Svetsaren*, **3**, 13–15.
9. Ericsson, M., Sandstrom, R. (2003) Influence of melting speed on the fatigue of friction stir welds, and comparison with MIG and TIG. *Int. J. Fatigue*, **25**, 1379–1387.
10. Enomoto, M. (2003) Friction stir welding: research and industrial applications. *Welding Int.*, **5**, 341–345.
11. Shtrikman, M.M., Polovtsev, V.A., Shilo, G.V. et al. (2004) Friction welding of sheet structures of aluminium alloys 1201 and AMg6. *Svarochn. Proizvodstvo*, **4**, 41–47.
12. Lanciotti, A., Vitali, F. (2003) Characterization of friction welded joints in aluminium alloy 6082-T6 plates. *Welding Int.*, **8**, 624–630.
13. Jata, K.V., Sankaran, K.K., Ruschau, J.J. (2000) Friction stir welding effects on microstructure and fatigue of aluminium alloy 7050-T7451. *Metallurg. Transact. A*, **31**, 2181–2192.
14. Kachanov, L.M. (1974) *Principles of fracture mechanics*. Moscow: Nauka.

METHODS FOR ASSESSMENT OF STRENGTHENING OF HSLA STEEL WELD METAL

V.A. KOSTIN, V.V. GOLOVKO and **G.M. GRIGORENKO**
E.O. Paton Electric Welding Institute, NASU, Kiev, Ukraine

Possibilities of application of strengthening mechanisms and structural approach to evaluation of strengthening of weld metal of high-strength low-alloyed (HSLA) steels were analyzed. It is shown that brittle fracture resistance of welds is mainly influenced by solid solution and grain-boundary strengthening.

Keywords: *arc welding, HSLA steels, weld metal, strengthening mechanisms, structure, forecasting mechanical properties*

At present HSLA steels are one of the most promising materials in welded structure fabrication. Starting from 1970s a lot of attention was given to investigations of the problems of metallurgy and technology of welding these steels. The accumulated extensive material on the properties of welded structures from this steel class allows forecasting the ways and the background technologies of further improvement of the entire set of mechanical properties of welds on HSLA steels. Analysis and generalization of the data of various researchers allowed defining several postulates aimed at producing reliable welded joints of HSLA steels with a high level of service properties [1, 2]. In particular, it is believed that in order to ensure an optimum combination of the values of strength, toughness and ductility of the metal of welds, made on HSLA with up to 560 MPa yield point, it is necessary to form wells with a high content of acicular ferrite structure [3, 4]. Investigations performed recently [5, 6] showed that an increased content of acicular ferrite in the weld structure in itself does not guarantee producing metal with high strength and toughness values. The process of brittle fracture, on the one hand, is influenced by solid solution alloying, and on the other hand — by the characteristics of non-metallic inclusions.

At evaluation of the influence of alloying on solid solution strengthening many authors used three main approaches: by metal composition, strengthening mechanisms and content of microstructural components.

In the first case, regression equations are used, which are based on the results of experiments on determination of metal mechanical properties, depending on the change of its alloying element content within certain limits. Such dependencies are valid only for that part of the compositions, for which they were established. So, the results of investigation of weldability of HSLA steels with C–Mn–Si alloying system [7] generalized in the equations

$$\sigma_t = 268 + 450[C + 0.33Si + Mn(1.6C - 0.145)], \quad (1)$$

$$a_I^{+20} = 144 - 387C + 330C^2 \quad (2)$$

cannot be used for low-alloyed steels with C–Mn–Si–Mo–Ni–Ti alloying system.

In the second case proceeding from the physical processes influencing the weld metal strengthening, an evaluation is proposed which is based on analysis of strengthening mechanisms, in keeping with which it is necessary to take into account the mechanism of solid solution, dislocation, dispersion and grain-boundary strengthening [8]. For instance, yield point $\Delta\sigma_y^F$ and temperature of transition from the brittle to tough fracture mode of ferritic-pearlitic steel T_{br}^{FP} can be determined as

$$\sigma_y^{FP} = \sigma_0 + \Delta\sigma_{s.s}^F + \Delta\sigma_{disl}^F + \Delta\sigma_P + \Delta\sigma_{d.str}^F + \Delta\sigma_{gr}^F + \Delta\sigma_{sub}^F, \quad (3)$$

$$T_{br}^{FP} = T_0 + (0.4–0.6)\Delta\sigma_{s.s}^F + 0.4\Delta\sigma_{disl}^F + \\ + 0.3\Delta\sigma_{d.str}^F - 0.7\Delta\sigma_{gr}^F, \quad (4)$$

where σ_0, T_0 are the initial strength and transition temperature of an iron single-crystal ($\sigma_0 = 2\cdot10^{-4}G$ ~ ~ 30 MPa); $\Delta\sigma_{s.s}^F$ is the solid solution strengthening at the expense of ferrite alloying; $\Delta\sigma_{disl}^F$ is the contribution of dislocation strengthening at the expense of dislocation density in ferrite; $\Delta\sigma_P$ is the pearlite strengthening at the expense of pearlite grain formation; $\Delta\sigma_{d.str}^F$ is the dispersion strengthening at the expense of disperse inclusions of carbides and nitrides in ferrite; $\Delta\sigma_{gr}^F$, $\Delta\sigma_{sub}^F$ is the grain boundary strengthening at the expense of the change of ferrite grain and subgrain size, respectively.

Contribution of various strengthening mechanisms can be given by the following system of equations:

$$\Delta\sigma_{s.s} = 4670[C] + 33[Mn] + 86[Si] + 82[Ti] + \\ + 30[Ni] + 11[Mo], \quad (5)$$

$$\Delta\sigma_{disl} = \alpha G b \rho^{1/2}, \quad (6)$$

$$\Delta\sigma_{gr} = \frac{k_y}{\sqrt{d}}, \quad \Delta\sigma_{sub} = \frac{k_y}{d}, \quad (7)$$

$$\Delta\sigma_{d.str} = (9.8\cdot10^3/\lambda)\ \ln 2\lambda, \quad (8)$$

$$\Delta\sigma_P = 2.4P, \quad (9)$$

where $\alpha = 0.5$, $k_y = 0.63$ MPa$\sqrt{m}$ are the coefficients for steel; $G = 84{,}000$ MPa for steel; $b = 2.5\cdot10^{-7}$ mm is the Burgers vector for steel; d is the average size of the ferrite grain or subgrain, μm; λ is the interparticle spacing having a strengthening effect on the solid solution; P is the pearlite fraction, %.

Development of the concepts of the mechanism of microstructural feature influence on solid solution strengthening and mechanical properties of the weld metal allowed defining one more method of assessment of the values of strength and ductility of welds, proceeding from the data on the number of microstructural components and their individual properties [9]. HSLA steels can be regarded as a polyphase mixture, the composition of which includes ferrite (F), pearlite (P), bainite (B) and martensite (M), secondary phases in the form of carbides and carbonitrides of microalloying elements, non-metallic inclusions (oxides, sulphides). If steel is to be considered as a natural composite of the above phases, then its strength properties (σ_y, σ_t) can be presented as a sum of strength properties of each component, multiplied by its volume fraction in the weld:

$$\sigma_y = \sigma_F V_F + \sigma_P V_P + \sigma_B V_B + \sigma_M V_M + \sum \sigma_{d.str\,i} V_{d.str\,i}, \quad (10)$$

where σ_F, σ_P, σ_B, σ_M are the volume fractions of ferrite, pearlite, bainite and martensite, allowing for their volume fractions V_F, V_P, V_B, V_M; $\sigma_{d.str\,i}$, $V_{d.str\,i}$ are the strength and fraction of secondary phase component in the weld metal.

The properties of each structural component, included into formula (1), are determined by the composition, morphology and dispersity of the structure. Strength of ferrite component σ_F is presented as a sum of three addends

$$\sigma_F = \Delta\sigma_{s.s}^F + \Delta\sigma_{disl}^F + \Delta\sigma_{gr}^F, \quad (11)$$

which are found by formulas (5)–(7), and pearlite strength σ_P — by expression (9).

Influence of the bainite component of the structure can be assessed using a linear dependence of strength in the range from the temperature of the start of bainite transformation B_s up to the temperature of maztensite formation M_s:

$$\sigma_B = \frac{(\sigma_F V_F + \sigma_P V_P)}{(V_F + V_P)} + \\ + \left[\frac{1}{V_M}\sum \frac{(B_s - T_i)}{(B_s - M_s)} \frac{\sigma_M - (\sigma_F V_F + \sigma_P V_P)}{(V_F + V_P)\Delta V_{B_i}}\right], \quad (12)$$

where T_i is the temperature of bainite transformation at i-th moment of time; ΔV_{B_i} is the increment of bainite volume during i-th time interval [10].

The main factor determining the strength properties of martensite is carbon content in martensite. The contribution of martensite component can be assessed by the formula from work [11]:

$$\sigma_M = A_M + B_M\sqrt{C}, \quad (13)$$

where A_M, B_M are the empirical components; C is the carbon content in martensite (MAC-phase).

According to Marder and Krauss, martensite strength is related to the dimensions of martensite packs, d_p, by a relationship of Hall–Petch type $\sigma_M = 449 + 60d_p^{-1/2}$, where σ_M is expressed in megapascals, d_p in micrometers.

Dispersion strengthening $\sigma_{d.str\,i}$ depends on the volume fraction and dispersity of secondary phases (carbide, carbonitride and non-metallic inclusions) and is given by the formula in (8).

Thus, knowing the composition of weld metal, volume fractions of primary (ferrite, pearlite, bainite and martensite) and secondary phases (carbide, carbonitride phases and non-metallic inclusions), dispersity and morphology of the structure, it is possible to reliably predict the mechanical properties of metal of HSLA steel welds.

Welded joints of HSLA steel were made in order to analyze the possibilities of application of strengthening mechanisms and structural approach to weld metal strengthening. Composition of base metal, welding wire and welds is given in [12].

Table 1. Quantity of microstructural constituents (%) and average size of ferrite grain d_f of weld metal alloyed by manganese

Weld designation	Acicular ferrite	Polygonal ferrite	Lamellar ferrite		Polyherdral ferrite	Side Widmanstaetten ferrite	d_f, μm
			With unordered second phase	With ordered second phase			
GA13G	49.5	2.0	17.0	5.0	26.5	0	360
GA09G	48.0	9.5	9.0	3.5	30.0	0	250
GA19G	61.5	13.5	3.0	0	22.0	0	150
GA13G2	55.0	7.5	17.5	2.5	15.5	1	300
GA09G2	64.5	8.0	0	0	25.0	2	250
GA19G2	85.0	4.0	0	0	8.0	3	170

Table 2. Quantity of microstructural coconsituents (%) and average size of ferrite grain d_f of the metal of welds alloyed by titanium

Weld designation	Acicular ferrite	Polygonal ferrite	Lamellar ferrite		Polyherdral ferrite	Side Widmanstaetten ferrite	d_f, μm
			With unordered second phase	With ordered second phase			
GA13T	23.5	10.5	21.5	7.5	29	8	150
GA09T	10.0	20.0	–	20.0	50	–	120
GA19T	6.0	3.7	55.0	33.0	2.3	–	70
GA13T2	7.0	9.0	41.0	9.0	–	–	100
GA09T2	–	5.7	36.7	57.6	34	–	70
GA19T2	–	2.0	25.3	71.7	1	–	50

During metallographic investigations the fraction of individual components of weld metal microstructure, elemental composition and distribution of non-metallic inclusions by size were determined. The microstructure was studied by the method of optical and electron metallography using light microscope «Neophot-32» and JEOL scanning electron microscope JSM-840, fitted with MicroCapture card for image capturing with subsequent recording of the image on the computer screen. Quantitative determination of microstructural components was conducted in keeping with IIW procedure.

Results of determination of microstructural composition of the metal of welds and average size of ferrite grain, obtained when studying ground samples in 4 % solution of nitric acid in ethanol, are given in Tables 1 and 2.

Analysis of the data on the quantity, volume fraction and size distribution of non-metallic inclusions, obtained at metallographic investigations of unetched sections, showed the existence of certain differences in the morphology of inclusions of different sizes. Finely-dispersed inclusions of up to 1.0 μn size have a nugget, consisting of aluminium and titanium oxides, and external fringe of a cubic shape with a high content of titanium nitrides (Figure 1, *a*). Larger inclusions consist of oxides of a complex composition, which have manganese sulphide precipitates on their surface (Figure 1, *b*).

Strengthening effect of the inclusion on the surrounding matrix is determined by the difference in the coefficients of thermal expansion of the inclusion and matrix. The contribution of secondary nitride or carbonitride phases to dispersion strengthening $\sigma_{d.str\ i}$

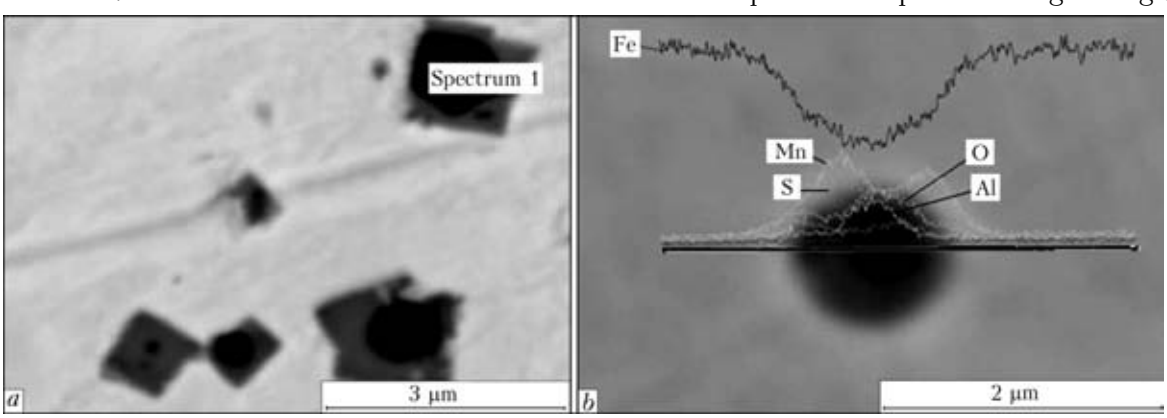

Figure 1. Morphology of non-metallic inclusions of less than 1.0 (*a*) and more than 1.5 (*b*) μm size

Table 3. Volume fraction of non-metallic inclusions, their size distribution and results of calculation of particle spacing λ by formula (8)

Weld designation	Volume fraction of inclusions, %	Content (%) /quantity (pcs) of inclusions in the dimensional range, μm					λ, μm
		< 0.3	0.5–1.0	1.25–2.0	2.25–3.0	> 3.0	
GA13G	0.83	32/761	45/1050	18/422	3/74	2/43	3.21
GA09G	0.24	37/558	49/735	11/169	1.5/22	1/16	3.09
GA19G	0.09	31/274	62/547	6.5/57	0.1/1	0/0	2.69
GA13G2	0.79	35/665	43/827	18/340	3/54	2/33	2.89
GA09G2	0.25	37/513	52/718	10/138	1/16	0.3/4	2.71
GA19G2	0.14	46/423	45/416	7/60	1/9	0.7/6	2.16
GA13T	0.40	25/243	51/490	17/159	5/45	3/26	3.96
GA09T	0.24	53/647	37/458	8/94	2/21	0.25/3	2.99
GA19T	0.12	33/233	52/360	11/79	3/21	0.6/4	1.89
GA13T2	0.65	53/408	33/258	10/75	3/21	1.5/12	1.89
GA09T2	0.35	56/315	35/197	2/10	1.5/8	1.5/8	1.80
GA19T2	0.23	62/386	30/189	6/36	2/11	0.16/1	1.61

is considerable, so that the matrix develops compressive forces around such inclusions, whereas for sulphides this value is significantly lower that promotes formation of ruptures on the inclusion-matrix interphase and practically complete absence of the influence of inclusions on weld metal properties [13].

During analysis and processing of metallographic images the fraction of non-metallic inclusions of not more than 1.0 μm size was calculated. Obtained data were used to calculate the values of interinclusion distances, λ, given in Table 3.

Based on the results of metallographic investigations (see Tables 1 and 2), calculations were performed by formulas (5)–(8) to determine the contribution of individual components to solid solution strengthening of weld metal. Pearlite influence on strengthening was not calculated in view of its absence in the weld structure. Proceeding from the reasons given in [14, 15], the contribution of dislocation strengthening (about 150–180 MPa) was taken to be constant, and it change during alloying by manganese and titanium was not considered.

Results of testing weld metal samples to GOST 6996 are given in Table 4, Figures 2 and 3 show the results of calculation of the contribution of solid solution, dispersion and grain-boundary mechanisms into strengthening of the studied weld metal and its comparison with the yield point and tensile strength.

Analysis of the obtained results shows that the greatest contribution to strengthening is made by grain-boundary and solid solution strengthening. Comparison of the calculated (Figure 3) and experimental data on tensile strength and yield point of weld metal (Figure 4) shows their reasonably good agreement. On the other hand, the observed deviations from the calculated and experimental results (in welds alloyed with large quantities of titanium) are due to the fact that titanium being a strong carbide-forming element starts interacting with carbon and nitrogen forming finely-dispersed carbides and carbonitrides, which, similar to oxide inclusions, have a strengthen-

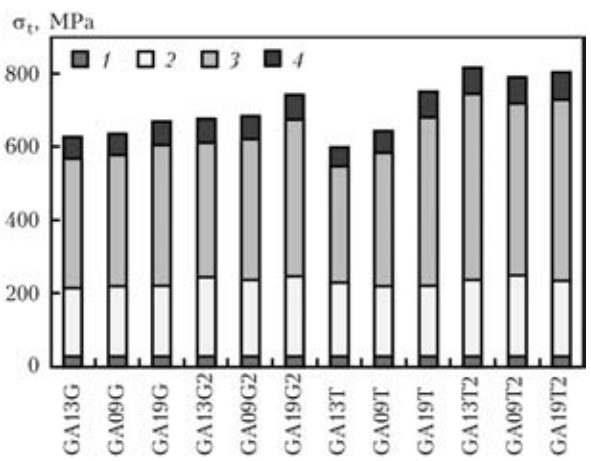

Figure 2. Calculated contribution of various strengthening mechanisms into the strength of the metal of welds alloyed by manganese and titanium: *1* — lattice friction; *2* — solid solution *3* — grain-boundary; *4* — dispersion strengthening,

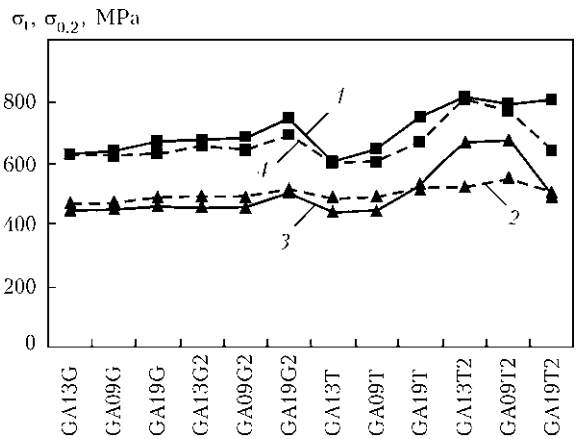

Figure 3. Comparison of calculated values (*1*, *2*) of tensile strength (σ_t) and yield point ($\sigma_{0.2}$) with their experimental (*3*, *4*) values obtained for the studied welds

Table 4. Mechanical properties of the metal of welds alloyed by manganese and titanium

Weld designation	$\sigma_{0.2}$, MPa	σ_t, MPa	δ_5, %	ψ, %	*KCV*, J/cm^2, at *T*, °C		
					20	0	−20
GA13G	446.4	626.2	21.0	59.9	47.3	31.9	20.8
GA09G	444.4	621.1	23.4	65.0	126.2	94.6	66.8
GA19G	458.8	627.9	22.3	67.9	144.1	107.7	94.2
GA13G2	453.8	652.8	21.2	57.5	58.0	41.4	29.9
GA09G2	455.2	638.9	23.4	64.0	98.4	78.0	60.1
GA19G2	501.0	686.7	21.8	64.8	103.9	69.4	53.5
GA13T	437.7	597.5	23.1	58.8	62.4	42.9	23.7
GA09T	443.4	603.5	23.5	67.7	64.3	40.8	19.0
GA19T	527.2	665.9	18.8	66.9	43.3	20.9	13.8
GA13T2	664.2	807.3	17.6	66.0	22.2	16.7	13.0
GA09T2	673.3	769.0	17.5	63.9	28.5	13.8	16.0
GA19T2	488.9	634.0	20.6	59.8	49.6	18.3	13.9

ing impact on the solid solution. Unfortunately, determination of the composition, size, distribution and spacing of carbides (8) requires performance of additional transmission electron microscopy investigations and X-ray spectral analysis.

Increase of weld metal alloying by manganese causes a lowering of the temperature range of ferrite transformations [12] and promotes formation of ferritic structure with grain size in the range of 170–260 μm (see Table 1). Non-metallic inclusions in welds in this case have predominant dimensions of up to 1.0 μm, and fraction of inclusions of 0.5–1.0 μm size is from 30 up to 45 % (see Table 3).

Lowering of the temperature of the start of $\gamma \rightarrow \alpha$ transformation suppresses the growth of grain-boundary ferrite and leads to reduction of the content of its allomorphous morphology in the weld metal. Formation of relatively large ferrite grains in combination with a high content of disperse (up to 1.0 μm) inclusions and lower temperature of the end of bainite transformation, promote intragranular nucleation of bainitic ferrite and formation of up to 85 % of ferritic structure of acicular morphology (see Table 1). It should be noted that with lowering of temperature interval of bainite transformation the width of ferrite needles increases from 80 up to 160 μm. The structure of wider needles shows twinning boundaries that causes an increase of acicular ferrite hardness and lowering of weld metal impact toughness, despite an increased content of this constituent in the structure [12].

Weld metal alloying by titanium does not influence the temperatures of the start of ferrite and bainite transformation, but raises the temperature of the end of the latter [12], thus leading to an essential refinement of ferrite grain size (see Table 2). Volume fraction of non-metallic inclusions in the weld metal decreases, but content of inclusions of not more than 0.3 μm size with a high content of carbonitiride phase, increases (see Table 3). Increase of the content of finely-dispersed carbide phase in the metal of welds alloyed by titanium led to growth of the centers of α-phase nucleation, on the one hand, and increase of the fraction of dispersion strengthening in formation of mechanical properties of weld metal, on the other. At increase of the density of intergranular boundaries distribution, they become more probable sites of ferrite structure growth in terms of energy, while the high contamination of the boundaries by non-metallic inclusions larger than 1.5 μm, promotes the start of these transformations in the high temperature region, resulting in formation of a structure of Widmanstaetten ferrite type. Increase of ferrite content in the metal of titanium-alloyed weld series, with second phase precipitations in the form of thin plates, is accompanied by increase of its structure microhardness and lowering of brittle fracture resistance [12].

Thus, brittle fracture resistance of HSLA steel weld metal is mainly affected by solid solution and grain-boundary strengthening. While in samples of titanium-alloyed series the adverse influence of solid solution strengthening was compensated by refinement of the grain structure from 200 to 100 μm, in samples of titanium-alloyed series the extremely high contribution of solid solution strengthening could not be neutralized even at the expense of grain refinement to 50 μm.

Increase of the content of finely-dispersed carbide phase in the metal of titanium-alloyed welds led to enhancement of the role of dispersion strengthening in formation of mechanical properties of weld metal. Apparently, such carbides promote formation of a dispersed structure in the region of high-temperature austenite decomposition. However, in the case of formation of high-temperature morphological forms of bainitic ferrite the welds have a low level of toughness. To increase weld metal toughness, it is necessary to

attempt to achieve formation of an increased content of low-temperature bainitic ferrite forms in their structure through alloying by elements increasing the austenite stability.

CONCLUSIONS

1. Application of the method of strengthening evaluation, which allows for the strengthening mechanisms, enables an adequate prediction of strength properties of HSLA steel weld metal.

2. At simulation of the composition of HSLA steel weld metal, in order to achieve high values of strength, ductility and toughness of welded joints, it is necessary to achieve an increase of the contribution of $\Delta\sigma_{d.str}$ and $\Delta\sigma_{gr}$ at limitation of $\Delta\sigma_{s.s}$. The structure of weld metal in this case will develop morphological forms of bainitic ferrite, while the presence of a dispersed carbide phase will promote formation of a fine-grained secondary structure.

1. Pokhodnya, I.K. (2008) Metallurgy of arc welding of structural steels and welding consumables. *The Paton Welding J.*, **11**, 54–64.
2. Fujita, Y., Nakanishi, Y., Yurioka, N. (2008) Advanced welding technologies in recent industries in Japan (Review). *Ibid.*, **11**, 40–45.
3. Lyakishev, N.P., Nikolaev, A.V. (2003) Metallurgy of steel: specifics of production in the XX century, problems and prediction of future development. *Ibid.*, **10/11**, 38–45.
4. Olson, D.L., Metzbower, E., Liu, S. et al. (2003) Developments in property predictions for weld metal. *Ibid.*, **10/11**, 31–37.
5. Grabin, V.F., Golovko, V.V. (2007) Effect of distribution of manganese in structural components on properties of low-alloy weld metal. *Ibid.*, **12**, 19–22.
6. Golovko, V.V., Grabin, V.F. (2008) Effect of alloying of high-strength weld metal with titanium on its structure and properties. *Ibid.*, **1**, 13–17.
7. Frantov, I.I., Stolyarov, V.I., Nazarov, A.V. et al. (1987) Optimization of composition of low-alloy welded steels. *Metallovedenie i Term. Obrab. Metallov*, **11**, 37–42.
8. Goldshtejn, M.I. (1987) Ways of increase in strength and cold resistance of structural steels. *Ibid.*, **11**, 6–11.
9. Young, C.H., Bhadeshia, H.K.D.H. (1994) Strength of mixtures of bainite and martensite. *Material Sci. and Technology*, 10(**3**), 209–214.
10. Mazur, V.L., Nogovitsin, A.V. (2010) *Theory and technology of sheet rolling (numerical analysis and technical appendixes)*. Dnepropetrovsk: Dnipro-VAL.
11. Liska, S., Wozniak, J. (1981) Matematisky model pro analyz v technologickyck podminek valcovani oceli za tepla. *Hutn. Actual*, 22(**9**), 1–49.
12. Golovko, V.V., Kostin, V.A., Zhukov, V.N. et al. (2010) Effect of alloying with manganese and titanium on peculiarities of decomposition of austenite in low-alloy weld metal. *Vesnik ChGTU*, **45**, 125–133.
13. Gubenko, S.I., Parusov, V.V., Derevyanchenko, I.V. (2005) *Non-metallic inclusions in steel*. Donetsk: Art-Press.
14. Vysotsky, V.M., Motovilina, G.D., Khlusova, E.I. (2004) Theoretical and experimental evaluation of strengthening and embrittlement of low-alloy ferritic-pearlitic steels. *Voprosy Materialovedeniya*, **4**, 5–13.
15. Schastlivtsev, V.M., Yakovleva, I.L. (2009) Principal structural factors of strengthening of low-alloy low-carbon pipe steels after controlled rolling. *Metallovedenie i Term. Obrab. Metallov*, **1**, 41–45.

ROLE OF NON-METALLIC INCLUSIONS IN CRACKING DURING ARC CLADDING

Yu.M. KUSKOV, D.P. NOVIKOVA and **I.L. BOGAJCHUK**
E.O. Paton Electric Welding Institute, NASU, Kiev, Ukraine

The effect of non-metallic inclusions in the base metal on initiation and propagation of cracks in the deposited metal is considered. It is shown that, in addition to the non-metallic inclusions, the propagation of cracks in the deposited metal is also promoted by the hardening phases present in its structure, as well as by the polygonisation boundaries. However, the latter are not the initiating factors of cracking.

Keywords: *base and deposited metals, non-metallic inclusions, cracks, hardening phases, polygonisation boundaries*

The optimal composition of a wear-resistant deposited metal is chosen experimentally or by mathematical modelling. The second variant is a better choice, as it is more cost-effective. However, as shown by practice, in many cases, especially in cladding of high-carbon steels, at a stage of verification of workability of a chosen cladding consumable the calculated «optimal» composition should be corrected to avoid cracks in the deposited metal. The use of this twofaced method of assessment of the investigation data results in formation of the final composition of the deposited metal. In this case, the technological part of the investigations is usually limited to studies of the processes taking place only in the deposited metal. Moreover, in view of some economical difficulties with purchasing of metal, the use is made of the «available» steels, although the provisions are made for conducting a high-quality chemical analysis of this metal.

This study is dedicated to investigation of the effect of quality of the base metal on the results of cladding, and in particular on the initiation of cracks in the deposited metal.*

Cladding was performed on specimens cut by the gas cutting method from the «available» rolled steel

*The study was carried out with participation of Dr. I.I. Ryabtsev.